# PREDICTION OF THE DYNAMIC RESPONSE OF A SHIP IN HEAD WAVES USING OPENFOAM TOOLBOX

(DOI No: 10.3940/rina.ijme.2020.a1.565)

**J Yao**, Key Laboratory of High Performance Ship Technology, Wuhan University of Technology, Ministry of Education, China

**SUMMARY**

Ships and marine structures, such as oil tanker, offshore platforms, etc., usually face extreme seaway environment in real situation. If under the action of strong waves large amplitude motions will occur, with the result that they may not work as usual or even lose stability. Thus, it is of great importance to access their dynamic responses under such bad conditions at the initial design stage, so as to ensure normal usage and safety. Herein, the original RANS (Reynolds-Averaged Navier-Stokes) solver based on OpenFOAM Toolbox has been extended to predict dynamic responses of ships and marine structures in waves. A new "inlet-velocity boundary condition" was implemented to generate waves. A damping term for wave absorption was added to the right-hand side of RANS equations in order to avoid wave reflection from the boundary where waves leave the computational domain. The related numerical methods are described in this paper. The purpose of this paper is to present a validation of the approach used. The prediction of the dynamic response of a ship in head waves was the focus. Five cases with different wave lengths and heights were considered. The predicted results, i.e. time histories of total resistance, heave and pitch, were compared with available experimental data and analysed. In addition, due to current experience it is very necessary that effort is devoted to determining appropriate grid and time step, so as to ensure the quality of waves generated.

## 1. INTRODUCTION

The hydrodynamic performances of ships and marine structures in waves are always of great interest. When a ship navigates in head waves, its speed will decrease compared with that in calm sea, because of added resistance. The magnitude of added resistance could reach 50% of the resistance in still water. Moreover, wave drift force will lead to position drift of a ship or marine structure, e.g. circle shift during a ship turning circle manoeuvre. These cause many problems, for example added resistance will increase greenhouse gas emission and trajectory shift results in difficulties in controlling ship. Besides, very strong waves will result in large-amplitude motions of ships and marine structures. If the motion amplitudes, such as rolling amplitude, exceed limiting values, they will lose stability and consequently overturn. For above reasons, designers should find optimum forms of ship hulls and marine structures to minimize negative impacts from waves as far as possible.

The response of ships and marine structures in waves is one of the major components in the research field of naval architecture and ocean engineering. The relevant problems, therefore, has been widely studied over a long time. Many studies on predicting the motions and hydrodynamics of ships and marine structures in waves have been reported in literatures. These studies were normally based on either EFD (Experimental Fluid Dynamics) or CFD (Computational Fluid Dynamics). Journée (1992) carried out experiments and calculations for four wigley hull forms in head waves. From the comparisons, it might be concluded that ship added resistance in regular waves, heave and pitch as well, reaches the peak around $\lambda \approx L$, where the wave frequency is near the condition of resonance. On the other hand, ship velocity affects the added resistance amplitude and resonance point, i.e. as increasing ship velocity the amplitude of added resistance usually becomes larger and resonance occurs at the condition of longer waves. The influence of ship velocity on heave and pitch shows a similar feature. Seo et al. (2013, 2014) predicted dynamic response for a various of ships by three potential approaches. Their study mainly focused on investigating the accuracy of approaches and showed reasonable agreement by comparison of computed results with EFD data.

Recently, viscous methods, especially RANS (Reynolds-Averaged Navier-Stokes), have gradually become popular for the study on hydrodynamics of bodies in waves. There are probably two reasons. One is that the methods are able to take viscous effects into account, which means the prediction accuracy will be higher than that based on potential approaches for the simulations of more complicated flow, e.g. turbulence around manoeuvring ships or bluff bodies. On the other hand, HPC (High Performance Computing) is now commonly able to afford the high computation cost. Relevant works of computing hydrodynamic forces by RANS have been reported by Guo (2012) and Sadat-Hosseini et al. (2013). In both studies, the response of a benchmark model named KVLCC2 was predicted. The method has been demonstrated to be of acceptable accuracy, in particular for the results of heave and pitch. The ship CFD workshop Tokyo 2015 released the benchmark EFD data for a container ship KCS in head waves. This offers a very good data source for validation of CFD computations and attract more interest from researchers.

OpenFOAM is an open source toolbox for CFD and has been developed to be available for applications in hydrodynamics

 

since the first version was released on 2004. Its ability and accuracy impress people on the workshop Tokyo 2015. The long-term objective of present study is to develop CFD techniques for predictions of hydrodynamic performance of ships and marine structures. Herein OpenFOAM is introduced to achieve the goal. A few works on simulations of ship PMM (Planar Motion Mechanism) tests for manoeuvring prediction has been carried out by the authors (Yao et al., 2016). A virtual piston-type wave maker has been developed as well (Yao, 2017). At present, the hydrodynamic problems related to waves are focused on. In this paper, the latest outcome concerning this aspect is presented. The purpose is to validate the new developed RANS solver. The approaches are described and simulations for KCS in head waves are performed. The computed results are validated by comparison with the EFD data from the workshop Tokyo 2015.

## 2. APPROACH

### 2.1 GOVERNING EQUATIONS

Considering a ship moves in ahead waves, the ship motion consists of forward linear motion and wave-excited heave and pitch. In order to describe the motion, a horizontal ship-fixed Cartesian coordinate system *o-xyz* is used, where the origin is located at the intersection of mid-ship sections and undisturbed free surface in still water, *x* axis toward bow, *y* axis towards starboard and *z* axis vertically downwards. It should be noted that the coordinate system moves together with the ship just in horizontal plane, and there exists relative motions between them, i.e. heave and pitch. OpenFOAM offers a method of mesh deformation for the simulation of relative motions.

Under the assumption of incompressible Newtonian fluid, the conservation equations of mass and momentum in above coordinate system can be written as

$$\frac{\partial U_i}{\partial x_i} = 0, \tag{1}$$

$$\frac{\partial U_i}{\partial t} + \frac{\partial (U_i U_j)}{\partial x_j} = -g_i - \frac{1}{\rho}\frac{\partial p}{\partial x_i} + \frac{\partial}{\partial x_j}\left[\nu\left(\frac{\partial U_i}{\partial x_j} + \frac{\partial U_j}{\partial x_i}\right) - \overline{U_i' U_j'}\right] + f_i, \tag{2}$$

where $\rho$ is the density of fluid, $\nu$ is kinematic viscosity, the subscripts $i, j$ and $k$ run from 1 to 3 denoting the three components of a quantity, $x_i = (x, y, z)$ and $U_i = (U, V, W)$ are independent Cartesian coordinates and flow velocity respectively, $g_i = (0,0,g)$ is the acceleration due to gravity, $f_i$ is momentum source term which can be used to dampen waves. According to Boussinesq hypothesis, the specific Reynolds stress tensor is assumed as

$$-\overline{U_i' U_j'} = \nu_t\left(\frac{\partial U_i}{\partial x_j} + \frac{\partial U_j}{\partial x_i}\right) - \frac{2}{3}\delta_{ij}k, \tag{3}$$

where $\nu_t$ is eddy viscosity, $k$ is turbulent kinetic energy and $\delta_{ij}$ is Kronecker symbol.

The $k$-$\omega$ SST turbulence model (Menter, 1994) with wall functions is employed to approximate the eddy viscosity in Eq. (3), where SST is the acronym of Shear-Stress-Transport and $\omega$ is specific dissipation rate. Since the model transport equations can be found everywhere and have been already described in a previous publication (Yao et al., 2016), they are not repeated here.

The two-phase flow (water and air) is dealt with by the available VoF (Volume of Fluid) method in OpenFOAM. The transport equation is

$$\frac{\partial F}{\partial t} + \frac{\partial (F U_i)}{\partial x_i} = 0, \tag{4}$$

where $F$ is the fraction function and physically represents that a computational cell with $F = 0$ is full of air, while if $F = 1$ it is full of water and when $0 < F < 1$ the cell locates at the interface between water and air. The density and viscosity in Eq. (2) are computed by

$$\rho = F\rho_w + (1 - F)\rho_a,$$
$$\nu = F\nu_w + (1 - F)\nu_a,$$

where subscripts $w$ and $a$ denote water and air respectively.

### 2.2 WAVE GENERATION

The method "inlet-velocity boundary condition (BC)" is used to generate waves. Although a dynamic BC for virtual piston-type wave makers can be employed, such kind of generating waves requires a lot of computational time due to the dynamic boundary and small time step, as reported by Yao (2017). The idea behind the "inlet-velocity BC" method is to superpose wave orbital velocity and wave elevation on the free-stream flow relative to the ship. Regular waves are considered in the simulations. Based on the linear wave theory, the wave profile in frame of the used coordinate system is written as

$$\zeta = -\zeta_a \sin(\omega_e t + k_w x), \tag{5}$$

then the components of wave orbital velocity are as follows

$$u_w = -\omega_0 a \frac{\cosh k_w(h-z)}{\sinh k_w h}\sin(\omega_e t + k_w x), \tag{6a}$$
$$v_w = 0, \tag{6b}$$
$$w_w = -\omega_0 a \frac{\sinh k_w(h-z)}{\sinh k_w h}\cos(\omega_e t + k_w x), \tag{6c}$$

where $h$ is water depth, $k_w$ is wave number, $\zeta_a$ is wave amplitude, $\omega_e$ is encounter frequency and expressed by

$$\omega_e = \omega_0 + k_w u_0, \tag{7}$$

where $u_0$ is ship speed and $\omega_0$ is wave circular frequency. Dispersion relationship is

$$\omega_0^2 = gk_w \tanh k_w h. \quad (8)$$

Note that the expressions of wave profile and orbital velocity are the ones when waves propagate along negative *x* axis.

Above expressions have been programmed based on the old BC named "fixed-Value" in OpenFOAM-v1612+. The new ones make it possible to set boundary values as a function of time and space, i.e. $t$ and $(x, y, z)$.

### 2.3 WAVE ABSORPTION

In present study, it must absorb waves downstream, avoiding wave reflection from boundaries behind ship. If not, the waves in the field will be disturbed, resulting in bad numerical accuracy. There are commonly two methods: add damping term in momentum equation or change cell size rapidly in the direction of wave propagation. Both are used here. Since it is only necessary to dampen wave height, the damping term, or here the source term in Eq. (2), is expressed as

$$f_i = (0,0,d(x)W), \quad (9)$$

where $d(x)$ is damping function, equal to zero except in the region of wave absorption. A liner damping law is applied, as

$$d(x) = \begin{cases} \alpha(x_s - x), & x \le x_s \\ 0, & \text{otherwise} \end{cases} \quad (10)$$

with $x_s$ the starting position of damping region and $\alpha(>0)$ an independent parameter which is adjusted to sufficiently absorb waves.

A C++ program block has been written to compute above damping term, which is coupled into the original OpenFOAM-based RANS solver.

Table 1 Particulars of KCS

| Particulars | | Full scale | Model scale |
|---|---|---|---|
| Length | $L_{pp}$[m] | 230 | 6.0702 |
| Beam | $B$ [m] | 32.2 | 0.8498 |
| Draught | $T$ [m] | 10.8 | 0.285 |
| Blockage | $C_B$ [-] | 0.651 | 0.651 |
| Longitudinal Centre of Buoyancy, fwd+ | $LCB$ [$\%L_{pp}$] | -1.48 | -1.48 |
| Vertical Centre of Gravity (from keel) | $KG$ [m] | 14.322 | 0.378 |
| Moment of Inertia | $K_{yy}/L_{pp}$[-] | 0.25 | 0.252 |

Table 2 Test Cases

| Wave Parameters | C1 | C2 | C3 | C4 | C5 |
|---|---|---|---|---|---|
| Length $\lambda$ [m] | 3.949 | 5.164 | 6.979 | 8.321 | 11.840 |
| Height $H_s$ [m] | 0.062 | 0.078 | 0.123 | 0.149 | 0.196 |

## 3. NUMERICAL RESULTS

### 3.1 CASES

The above approaches are applied to predict the response of KCS in head waves. The simulations are performed at model scale. Ship particulars at model and full scale are listed in Table 1. The ship speed considered at model scale is 2.017 m/s, corresponding to a Froude number 0.26 and Reynolds number $1.07 \times 10^7$. Five cases summarized in Table 2 are simulated. The cases are numbered from C1 to C5.

### 3.2 GRID AND BOUNDARY CONDITIONS

Unstructured grids generated by the software Hexpress are used for the simulations. Due to the symmetric flow, only half ship hull is considered. The computational domain is limited inside a box with the size of $-5 \le x/L_{pp} \le 1$, $0 \le y/L_{pp} \le 2$ and $-1 \le z/L_{pp} \le 1$. The domain length is around 3 times of wave length for C5. Figure 1 presents a sample mesh in the symmetric plane. As seen, in order to capture well wave features grid refinement is carried out near free surface. In the region $x/L_{pp} \le -1$, the cell size is enlarged rapidly along the direction of wave propagation until reaching the maximum set size, of which the purpose is to dampen waves as mentioned in section 2.3.

Five types of BCs are involved. The details are as follows.

(1) Wall BC: the wall BC, i.e. non-slip BC, is imposed on hull surface;
(2) Slip BC: the boundaries at $z/L_{pp} = \pm 1$, $y/L_{pp} = 2$ are considered as slip planes;
(3) Symmetry BC: due to the symmetric flow the boundary at $y/L_{pp} = 0$ is specified as a symmetric plane;
(4) Outlet BC: the boundary downstream at $x/L_{pp} = -5$ is set as outlet;
(5) Inlet BC: the flow velocity, i.e. $(u_w - u_0, v_w, w_w)$, and wave evaluation, i.e. $\zeta$, are imposed on the boundary in front of ship at $x/L_{pp} = 1$.

### 3.3 CHECKING OF WAVE QUALITY

Before performing the simulations of the ship in waves, wave quality is firstly checked since high-quality wave profile usually depends on the numbers of cell in both a wavelength and wave height, and also time step. Here the influences are investigated only for C1 because the wave height is smallest, length as well. For this purpose, a set of grids without ship hull are generated for isolated simulations of wave generation. Those empty grids are quite similar with the one (e.g. the one shown in Figure. 1) including ship geometry, i.e. the same domain size and size distribution of cells. Waves are absorbed in the region $x/L_{pp} \le -1$ and the parameter $\alpha$ is set to 5

[$m^{-1}s^{-1}$] according to a few pre-computations. In addition, BCs and other numerical settings are kept same too.

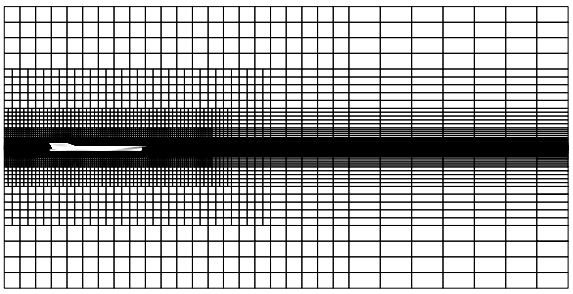

Figure 1: A mesh in the symmetric plane

A comparison of wave profiles using different grids (being refined systematically) is shown in Figure 2, where "4-64-0.002" denotes that there are around 4 cells in a wave height, around 64 cells in a wavelength and time step is 0.002 second and other notations represent the same meanings. The numbers of cell range from 0.46 to 14.9 million.

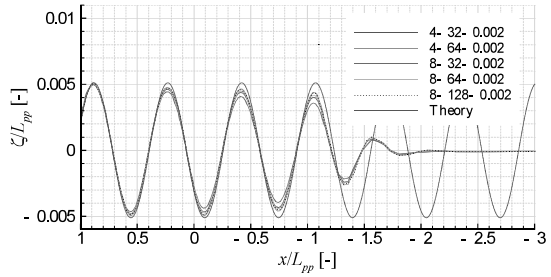


Figure 2: Comparison among wave profiles using different grids for C1

We note at the first glance that grid density affects only the wave attenuation, but not the phase. In the region $x/L_{pp} < -1$ wave amplitude is reduced rapidly, due to the damping term in Eq. (2) and rapid enlargement of cell size as described previously.

The comparison between the profiles based on "4-32-0.002" and "4-64-0.002" or "8-32-0.002" and "8-64-0.002" shows that when doubling the number of cell in a wavelength wave attenuation is reduced to a certain extent. Whereas, when doubling the number of cell in a wave height, the quality of profile becomes even worse (see the profiles based on "4-32-0.002" and "8-32-0.002" or "4-64-0.002" and "8-64-0.002"). If doubling both the profile is improved, as compared the profiles based on "4-32-0.002" and "8-64-0.002" or "4-64-0.002" and "8-128-0.002". The profiles based on "4-64-0.002" and "8-128-0.002" are very close and the closest ones to theory. It seems the wave quality is affected by the ratio of cell numbers in a wavelength and wave height.

To investigate the influence of time step on wave quality, another two simulations are performed for "4-64-0.002", but the time step is changed from 0.002 second to 0.001 and 0.004 second. The predicted profiles are presented in Figure 3. As observed, the time step affects only wave attenuation, but not the phase, which is also found when analysing the influence of grid density on wave profile. The wave profile becomes closer to theory when decreasing time step, as expected. The profile based on "4-64-0.001" is acceptable, at least in the region of interest, i.e. $-0.5 \leq x/L_{pp} \leq 0.5$, where the ship is located. The time history of wave evaluation at the centre of the ship is compared with theory in Figure 4. Figure 5 shows a snapshot of wave surface.

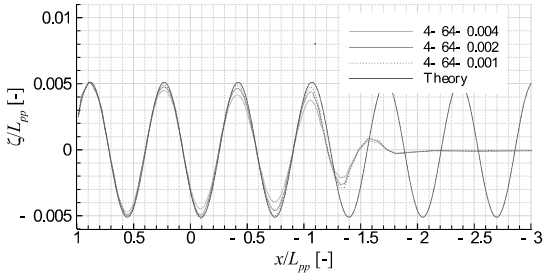


Figure 3: Comparison among wave profiles using different time steps for C1

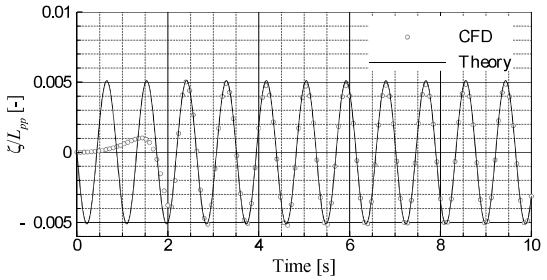


Figure 4: Time history of wave evaluation at the centre of ship

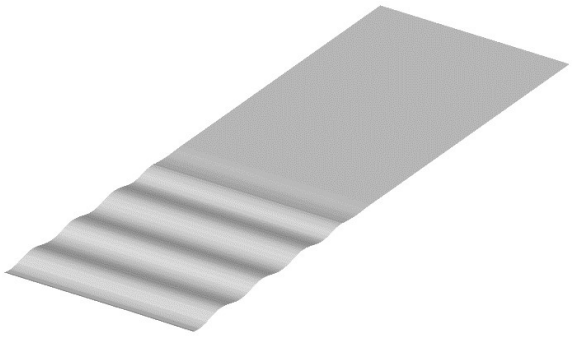

Figure 5: A snapshot of wave surface for C1 without ship hull

According to above checking of wave quality "4-64-0.001" should be preferred to be used. However, it remains worth checking wave profiles for other cases, since cell numbers in a wavelength and wave height, as well as encounter period, are different. For this reason, other four simulations are performed to generate the waves of C2 to C5 using the same grid and time step, i.e. "4-64-0.001" as

for C1. The predicted wave profiles are also in accordance with theoretical ones (not shown here), meaning that the grid and time step are suitable for all cases.

### 3.4 SIMULATION OF KCS IN HEAD WAVES

Simulations for C1 are firstly performed using two grids with ship geometry. The coarse one is generated based on "4-64", the fine one based on "8-128". The spacing of first grid point to hull surface is adjusted to agree the use condition of wall functions. For the simulations, the functionality of wave generation is inactive at beginning until the flow reaches steady state in still water. It should be noted that for the forepart still-water computation the time step is set to 0.02 second, then changed to 0.001 second when activating the module of wave generation. The computed $y^+$ along ship hull varies from around 40 to 220.

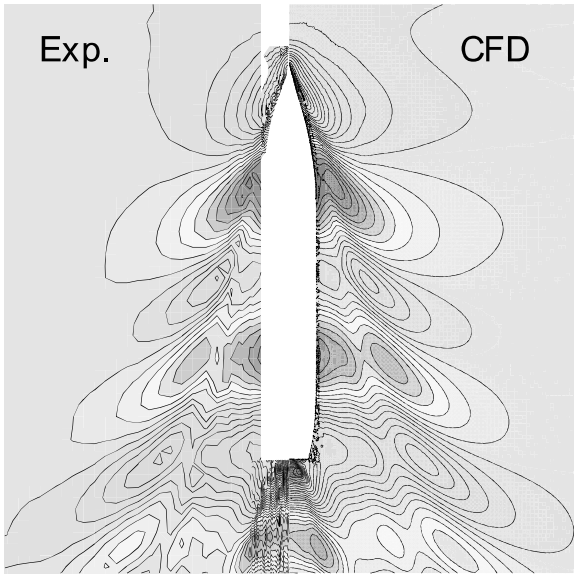


Figure 6: Comparison of computed wave evaluation with experiment in still water

The computed resistance, sinkage and trim in still water, as well as experimental data, are presented in Table 3, where $C_T$ is resistance coefficient (resistance is made non-dimensional by water density, ship velocity and wetted surface area of hull), $Z_s$ is sinkage and $\theta$ is trim. The difference between the results based on the coarse and fine grid is quite small, less than 1%. All numerical results agree well with EFD data. The errors are generally around 5%. The predicted wave evaluation based on the coarse grid in still water is compared with experimental one, as shown in Figure 6. The prediction captures well the main features of wave system.

The time histories of total resistance over one encounter period based on the coarse and fine grids are compared in Figure 7. It is clear that they are quite close. Although the cell size is almost made half and cell number becomes from around 2.9 million to 18.3 million, total resistance is not affected significantly, which indicates if refining the grid further significant influence on the results should not occur. On the other hand, the computation based on the fine grid requires around 45 days to run 10 encounter periods (the period is 0.887 second for C1), using 24 processes. So that, according to the synthesis consideration of computational time and accuracy, the coarse grid is employed for C2 to C5.

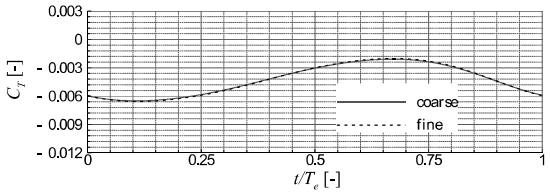


Figure 7: Time histories of total resistance based on the coarse and fine grid for C1

The computed time histories of total resistance for C1 to C5 are validated by comparison with EFD data, as shown in Figure 8. The result for C3 is not presented in the figure due to the unavailable EFD data. It can be seen that the computations underestimate the magnitudes of resistance for C1 and C2, whereas for C5 the computed curve agrees well with EFD. The EFD time history of C4 shows an oscillation, unlike the computed one. The phases of all computed curves are in complete agreement with EFD.

The computed time histories of heave and pitch are compared with EFD in Figures.9 and 10 respectively. The heave is predicted quite well as only small difference is found. For pitch, except for C2 other predictions achieve good results.

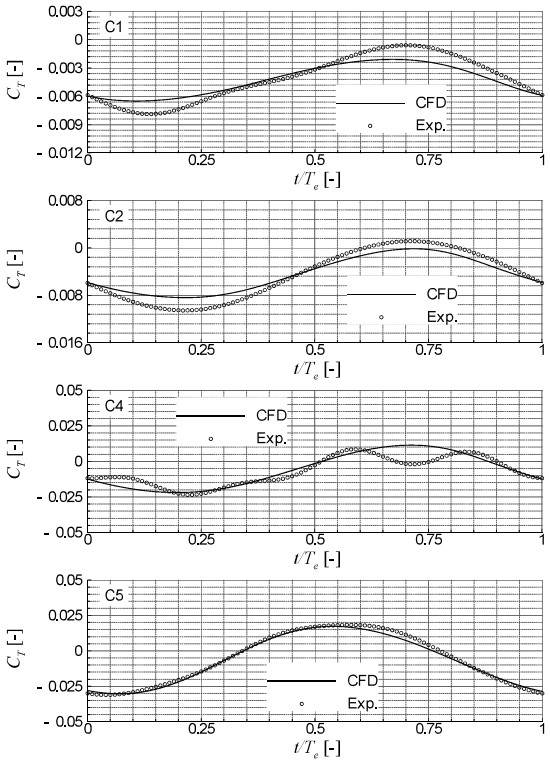


Figure 8: Validation of total resistance

The present results are similar to those presented by most participants on the workshop Tokyo 2015. Although the heave and pitch are generally predicted well, the prediction accuracy of resistance is not so ideal. It should point out that the present computations are performed under the "fixed-surge" condition. The seakeeping test in towing tank, however, was conducted using a spring system in surge direction, according to the recommended procedure of seakeeping committee ITTC (International Towing Tank Conference). The different condition for surge between EFD and CFD may be a main error source. In addition, for C1 and C2 the amplitudes of total resistance are relative small. The authors argue that the test error caused by facility is probably not small relative to the real value, which means the test uncertainty is large for C1 and C2. The EFD resistance for C4 is most probably wrong although the total tendency is in accordance with CFD, since the oscillations should not happen in theory.

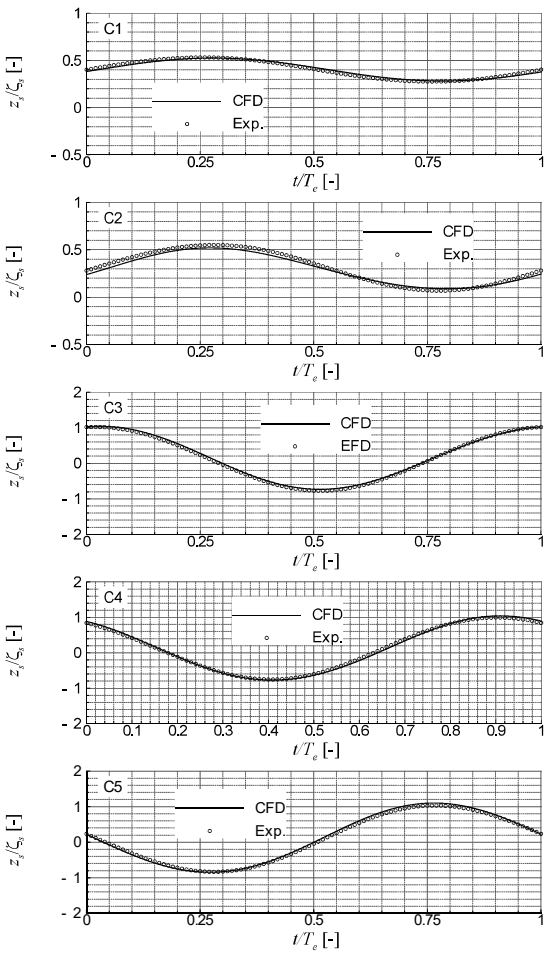


Figure 9: Validation of heave

Figure 11 presents the snapshots of wave surface. The wave patterns should be reasonable. It is valuable to the observation of wave reflection from hull surface. Due to the reflection, the free-stream wave right ahead of the ship hull is disturbed, which can be more clearly seen in pictures C3 and C5. For other cases, the reflection is also noticed, but relatively weaker. When reflected waves reach the inlet boundary, the flow velocity and wave elevation are forcedly changed into the prescribed free-stream boundary values. On the other hand, wave reflection from the side boundary can also occur. For this reason, the magnitude of total resistance oscillates periodically and slightly, as shown in Figure 12. The wave reflection is unavoidable during the computations, at least when using the approach "inlet-velocity BC" for wave generation.

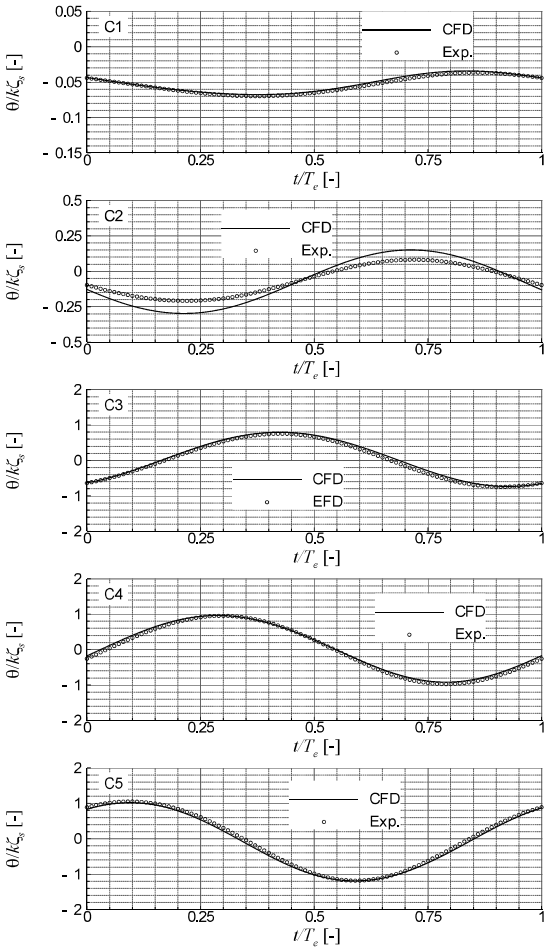


Figure 10: Validation of pitch

## 4. CONCLUDING REMARKS

This paper presents a study on predicting dynamic response of a ship in head waves using the RANS solver based on OpenFOAM. The methods, in particular about wave generation and absorption, are described in detail. In general, the computations show promising results, according to the comparison with EFD data. However, great efforts are required to ensure wave quality, which depends strongly on the grid and time step. Thus, a few

pre-computations are usually necessary to determine the appropriate grid and time step for considered waves.

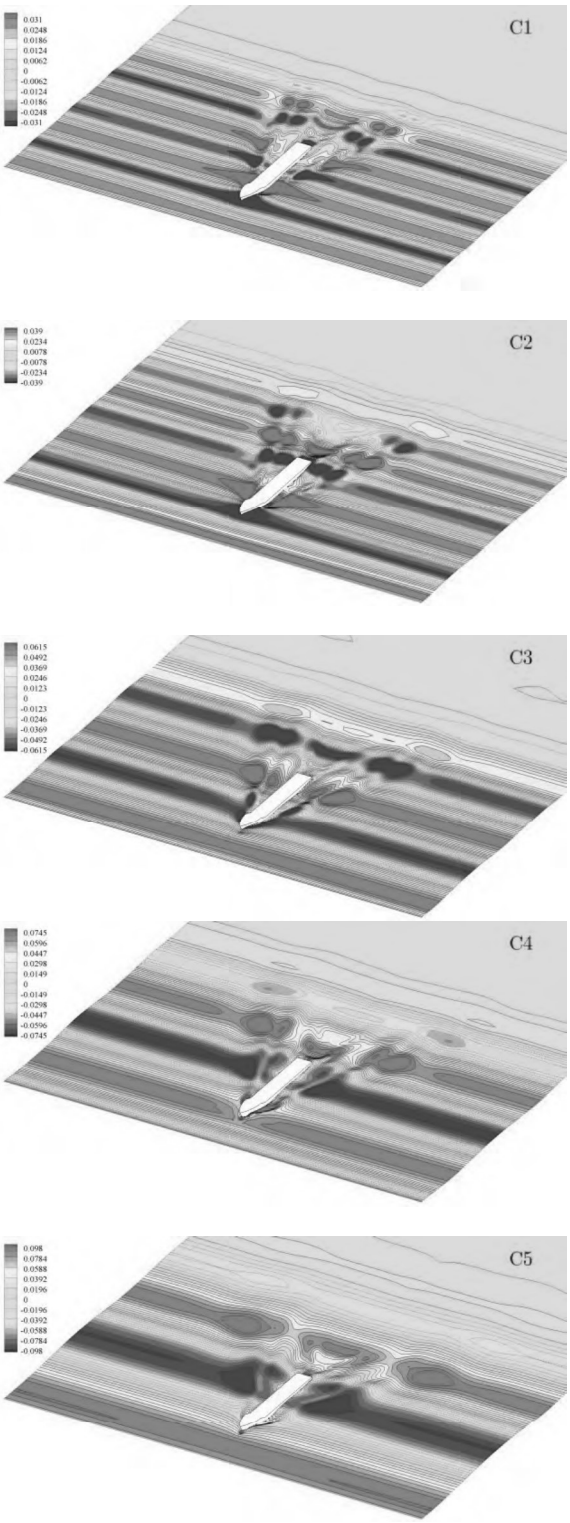


Figure 11: Snapshots of wave surface for C1 (top) to C5 (bottom)

Traditionally, many wave-related hydrodynamic problems can be successfully addressed by a method based on potential theory, e.g. panel method. For the problems concerning the simulations of more complex flows, e.g. a ship manoeuvring in waves, the advantage of RANS approach is clear. Although using RANS code is expensive in computational time, it is likely to become more popular for such simulations, as improved High Performance Computing (HPC) capabilities continue to be applied to CFD based simulations.

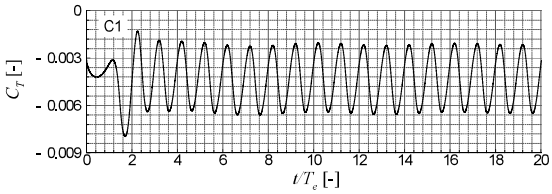


Figure 12: Time history of total resistance

## 5. ACKNOWLEDGEMENTS

This work was supported by National Natural Science Foundation of China (Grant No. 51609188, 51609187, 51609186, 51479150, 51709213, 51720105011) and Fundamental Research Funds for the Central Universities (WUT: 2016IVB006, 2017IVB007).

## 6. REFERENCES

1. GUO, B. J., STEEN, S. and Deng, G. B. (2012), *Seakeeping prediction of KVLCC2 in head waves with RANS*, Applied Ocean Research, 35: 56-67.
2. JOURNÉE, J. M. J. (1992), *Experiments and calculations on 4 Wigley hull forms in head waves*, Report 0909, Delft University of Technology.
3. MENTER, F. R. (1994), *Two-equation eddy-viscosity turbulence models for engineering applications*, AIAA J. 32(8): 1598-1605.
4. *Proceeding of the Workshop on CFD in Ship Hydrodynamics-Tokyo 2015*.
5. SEO, M. G., Yang, K. K., et al. (2013), *Comparative study on computation of ship added resistance in waves*, Ocean Engineering, 73:1-15.
6. SEO, M. G., Yang, K. K., et al. (2014), *Numerical analysis of added resistance on ships in short waves*, Ocean Engineering, 87: 97-110.
7. SADAT-HOSSEINI, H., Wu, P. C., et al. (2013), *CFD verification and validation of added resistance and motions of KVLCC2 with fixed and free surge in short and long head waves*, Ocean Engineering, 59: 240-273.
8. YAO, J., Jin, W. and Song, Y. (2016), *RANS simulation of the flow around a tanker in forced motion*, Ocean Engineering, 127: 236-245.
9. YAO, J. (2017), *A virtual piston-type wave maker based on OpenFOAM*, International Journal of Maritime Engineering, 159: 159-165.

 